Electronic Supplementary Material (ESI) for Journal of Materials Chemistry C.

Supporting Information

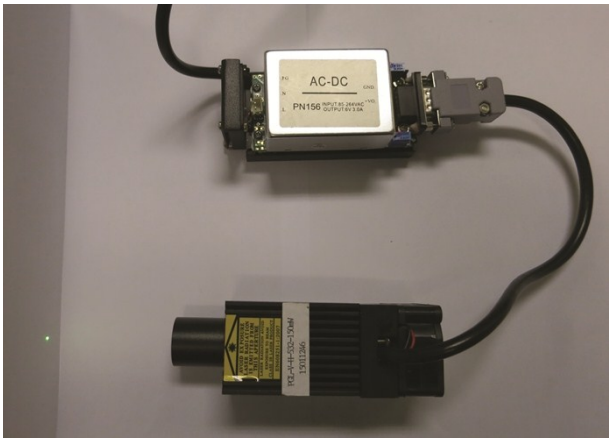

Fig. S1 Photograph of 532 nm laser.

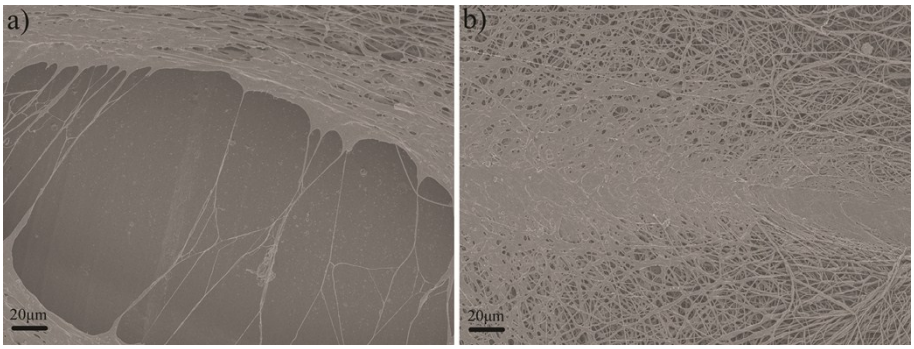

Fig. S2 SEM images of a) Au@PCL and b) Au@PCL$_x$ FMs with a typical crack after 532 nm light irradiation.

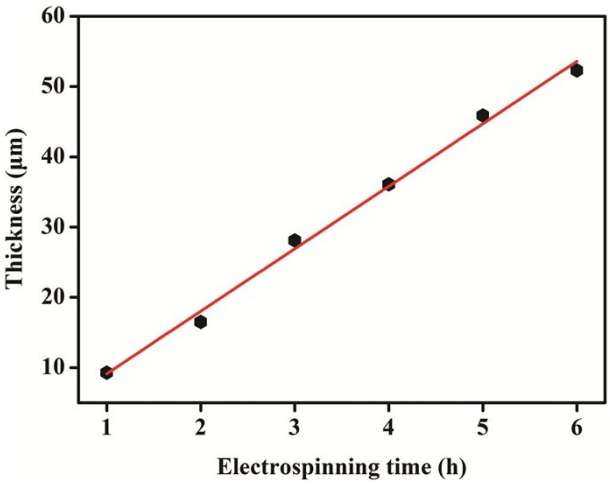

Fig. S3 Dependence of Au@PCL$_x$ FM thickness on electrospinning time.

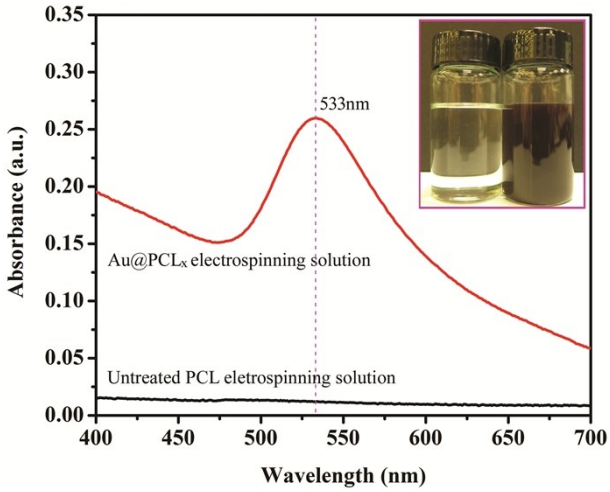

Fig. S4 UV-Vis absorption spectra of untreated PCL and Au@PCL$_x$ electrospinning solution; Inset shows the photograph of untreated PCL (left) and Au@PCL$_x$ (right) electrospinning solution.

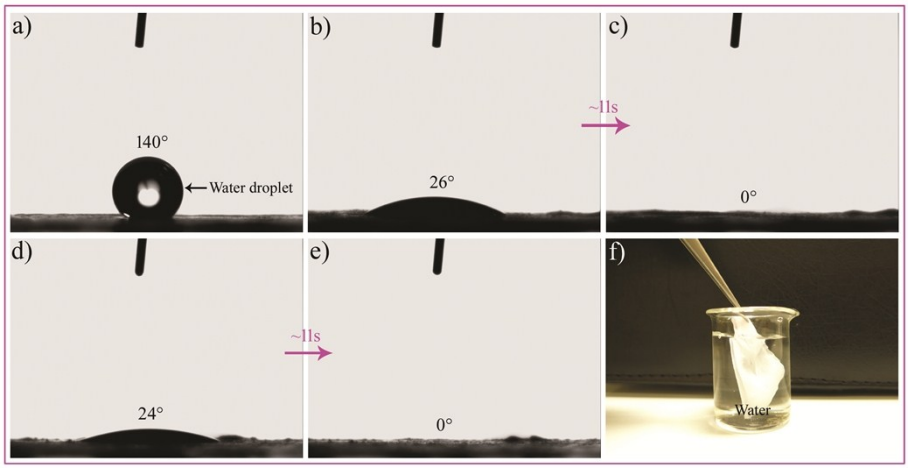

Fig. S5 a)-e) Photographs of water droplets on different PCL FMs: a) untreated PCL; b), c) PCL_x and d), e) $Au@PCL_x$. f) Photograph of $Au@PCL_x$ FM immersed in water.

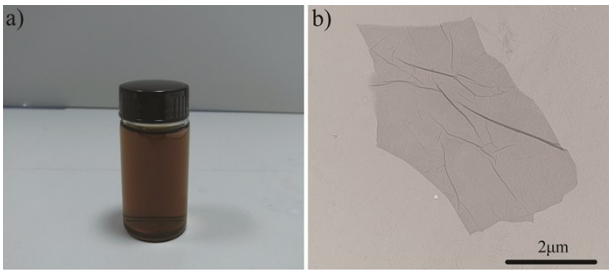

Fig. S6 a) Photograph of GO dispersion (1 mg/mL) and b) TEM image of GO.

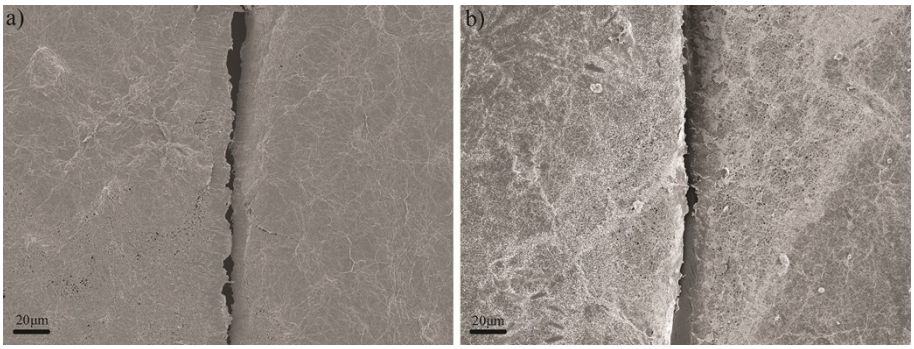

Fig. S7 SEM images of PCL_x/rGO and PCL_x/rGO/Ag FMs with a typical crack after 532 nm light irradiation.

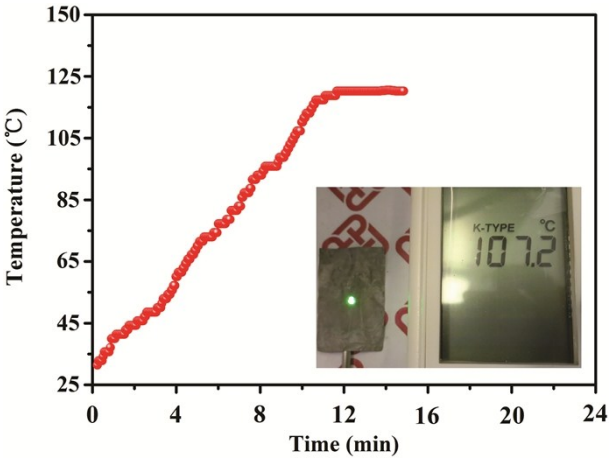

Fig. S8 Temperature versus time evolution of Au@PBS_x/rGO/Ag FM after 532 nm light irradiation.

Fig. S9 Photograph of the optically healed Au@PCL$_x$/rGO/Ag FM (marked by frame) withstanding a load >14 000 times its weight.

Table S1 Changes in mechanical properties of Au@PCL_x/rGO/Ag FM before cutting and after self-healing.

Samples	Tensile strength (MPa)	Elongation at break (%)	Tensile strength retention ratio (%)
Before cutting	4.85	103.3	100
After one cutting-healing cycle	4.4	95.7	90.7
After five cutting-healing cycles	3.35	51.4	69.1
After nine cutting-healing cycles	2.69	45.3	55.5